Multiple Pathways Act Together To Establish Asymmetry of the Ventral Nerve Cord in *Caenorhabditis elegans*

Jesse Taylor and Harald Hutter[1]
Department of Biological Sciences, Simon Fraser University, Burnaby, British Columbia V5A 1S6, Canada

ABSTRACT The central nervous system of most animals is bilaterally symmetrical. Closer observation often reveals some functional or anatomical left–right asymmetries. In the nematode *Caenorhabditis elegans*, the most obvious asymmetry in the nervous system is found in the ventral nerve cord (VNC), where most axons are in the right axon tract. The asymmetry is established when axons entering the VNC from the brain switch from the left to the right side at the anterior end of the VNC. In genetic screens we identified several mutations compromising VNC asymmetry. This includes alleles of *col-99* (encoding a transmembrane collagen), *unc-52*/perlecan and *unc-34* (encoding the actin modulator Enabled/Vasodilator-stimulated phosphoproteins). In addition, we evaluated mutants in known axon guidance pathways for asymmetry defects and used genetic interaction studies to place the genes into genetic pathways. In total we identified four different pathways contributing to the establishment of VNC asymmetry, represented by UNC-6/netrin, SAX-3/Robo, COL-99, and EPI-1/laminin. The combined inactivation of these pathways in triple and quadruple mutants leads to highly penetrant VNC asymmetry defects, suggesting these pathways are important contributors to the establishment of VNC asymmetry in *C. elegans*.

KEYWORDS asymmetry; central nervous system; ventral nerve cord; axon guidance

MOST animals are bilaterally symmetrical. This is considered a basic evolutionary trait and hence those animals are grouped together as Bilateria. Nevertheless, many bilaterians exhibit invariant left–right asymmetries in certain aspects of their anatomy, *e.g.*, in the location of unilateral internal organs such as the heart in vertebrates. In the nematode *Caenorhabditis elegans*, the most prominent asymmetry is the location of the gonad and the gut. In the anterior part of the animal, the gonad is always on the right side whereas the gut is on the left side (Wood 1998). The initial asymmetry is established early in the embryo when the daughters of the anterior AB blastomere, ABa and ABp, divide along the left–right axis at the four-cell stage. During the divisions, the spindles of ABa and ABp are skewed such that the daughter cells on the left side end up lying anterior to the respective sister cells on the right side (Sulston *et al.* 1983). The asymmetry gradually diminishes during embryogenesis as cells divide and mostly assume bilaterally symmetrical positions. Reversal of handedness at the six-cell stage by micromanipulation leads to normally developing animals with all left–right asymmetries completely reversed, suggesting that the symmetry-breaking event at this stage is responsible for all observed left–right asymmetries (Wood 1991).

A number of asymmetries are found in the nervous system. These relate to the positioning of cells and axons as well as distinct differentiation programs of symmetrically positioned neurons. Some of these asymmetries are primary, whereas others are secondary asymmetries developing from an initially symmetrical situation. The majority of the neurons (198 out of 302 in the hermaphrodite) form bilaterally symmetrical pairs (White *et al.* 1986). Many of the neurons not forming bilateral pairs, most notably motor neurons in the ventral nerve cord (VNC), are located at the ventral midline. Several unilateral neurons are also located at or close to the ventral midline.

Two bilaterally symmetrical pairs of sensory neurons, ASE right (ASER)/left (ASEL) and AWC right (AWCR)/left (AWCL), show molecular and functional differences (Hobert 2014; Alqadah *et al.* 2018). ASE neurons display directional

doi: https://doi.org/10.1534/genetics.119.301999
Manuscript received November 20, 2018; accepted for publication February 15, 2019; published Early Online February 21, 2019.
[1]Corresponding author: Department of Biological Sciences, Simon Fraser University, 8888 University Dr., Burnaby, BC V5A 1S6, Canada. E-mail: hutter@sfu.ca

asymmetry, with the left and right cells invariably expressing the same distinct fates. In contrast, the AWC neurons show stochastic asymmetry, with both subtypes (AWC^{ON} and AWC^{OFF}) having an equal chance of being on the left or on the right side. The AWC subtype decision is made during late embryogenesis and requires communication between the two AWC neurons (Troemel *et al.* 1999; Bauer Huang *et al.* 2007; Chuang *et al.* 2007). The asymmetry of the ASE neurons can be traced back to molecular asymmetries present at the six-cell stage in the different ASER and ASEL lineages (Chang *et al.* 2003, 2004; Cochella and Hobert 2012). This asymmetry is therefore a direct consequence of the initial symmetry-breaking event in the early embryo.

One pair of bilaterally symmetrical neuroblasts shows asymmetrical migration patterns on the left and right side. On the left side, the QL neuroblast and its descendants migrate posteriorly, whereas on the right side the QR neuroblast and its descendants migrate anteriorly (Sulston and Horvitz 1977). QR and QL produce bilaterally symmetrical neurons, *e.g.*, the touch neurons AVM and PVM. The different location (anterior *vs.* posterior) of AVM and PVM is thought to broaden the receptive field of these sensory neurons (Hobert *et al.* 2002).

Most axon tracts in *C. elegans* are bilaterally symmetrical. The notable exception is the VNC, which contains the main components of the motor circuit controlling movement of the animal. The VNC consists of two axon tracts flanking the ventral midline. The right axon tract contains ~50 axons, whereas the left axon tract contains only four axons (White *et al.* 1976). The asymmetry arises when interneuron axons approaching the VNC on the left side cross the midline to enter the right axon tract at the anterior end of the VNC. In this article, "establishment of VNC asymmetry" refers to this decision of axons to cross into the right VNC axon tract. "Failure to establish the asymmetry" or "loss of asymmetry" refers to the phenotype where axons fail to cross and remain on the left side instead (Figure 1).

The first neuron to send an axon into the VNC, AVG, invariably does so on the right side, thereby establishing the right axon tract (Durbin 1987). AVG is located at the anterior end of the VNC, close to the point where interneuron axons switch into the right axon tract. This makes the AVG axon an obvious candidate to establish the asymmetry. However, when AVG is either physically ablated or fails to differentiate properly (as in *lin-11* mutants), VNC asymmetry is still intact in the majority of animals (Hutter 2003). While AVG fails to differentiate properly in 100% of *lin-11* mutants, asymmetry defects caused by interneuron axons failing to cross from left to right as they enter the VNC occur in only 11% of mutant animals (Hutter 2003). This work suggests that AVG is not essential in the establishment of asymmetry. The RIF neurons are located next to the AVG neuron. Their axons cross the ventral midline at the position where interneuron axons cross into the right axon tract (Figure 1). RIF axons pioneer the pathway between the ventral cord and the nerve ring and could guide interneuron axons into the right axon tract. However, ablation of the RIF neurons does not cause any defects in establishing the VNC asymmetry (Hutter 2003). This suggests that interneuron axons can distinguish left and right sides in the absence of the pioneer axons, indicating that molecular cues present in the local environment might be important.

The guidance cue UNC-6/netrin is expressed in a gradient along the dorsoventral axis, with the highest concentration at the ventral side. The peak of expression is skewed slightly toward the right side since AVG expresses *unc-6* (Wadsworth *et al.* 1996). This led to the hypothesis that UNC-6 provides an asymmetrical cue to establish VNC asymmetry (Wadsworth *et al.* 1996). However, in *unc-6* mutants the VNC asymmetry is largely intact with only 8% of the mutant animals showing asymmetry defects (Hutter 2003). Currently the molecular basis for the establishment of VNC asymmetry is not well understood.

In this study we employed different strategies to identify the genes controlling VNC asymmetry in *C. elegans*. We first used direct genetic screens to isolate mutants with VNC asymmetry defects. This identified alleles of *col-99*, *unc-52*, and *unc-34*. All mutants isolated in these screens have weakly penetrant asymmetry defects, suggesting that several redundant pathways contribute to this process. We then employed a candidate gene approach to determine if known axon guidance signaling pathways contribute to VNC asymmetry. We thus identified four different pathways that act together to establish VNC asymmetry. The penetrance of asymmetry defects when multiple pathways are inactivated in triple and quadruple mutants approaches 80%, suggesting that we have identified several essential pathways controlling this process.

Materials and Methods

Strains and transgenes

The following alleles were used for phenotypic characterization: *unc-40(e271)* I, *unc-73(ev802)* I, *unc-73(rh40)* I, *unc-52(e444)* II, *unc-52(gk3)* II, *unc-52(hd133)* II, *vab-1(dx31)* II, *col-99(hd130)* IV, *unc-5(e53)* IV, *epi-1(rh200)* IV, *unc-34(hd132)* V, *nid-1(cg119)*, *ddr-1(ok874)* X, *ddr-2(ok574)* X, *nid-1(cg119)* V, *sax-3(ky123)* X, and *unc-6(ev400)* X.

The following integrated GFP reporter constructs were used to analyze axonal trajectories and neuronal cell body positions: *evIs111*[*rgef-1*::GFP; *dpy-20(+)*] V and *rhIs13*[*unc-119*::GFP; *dpy-20(+)*] V. Animals were cultivated at 20° under standard conditions (Brenner 1974) unless otherwise noted.

Genetic screens

Forward genetic screens were done using transgenic strains containing the pan-neuronal GFP-expressing reporter *evIs111* in a *rol-6* mutant background. Mutagenesis was performed as published (Brenner 1974) with the following modifications: For mutagenesis, L4 hermaphrodites were treated with 20 μl EMS in 4 ml M9 + $MgSO_4$ for 1 hr at room temperature. Tubes were rotated every 15 min to prevent suffocation.

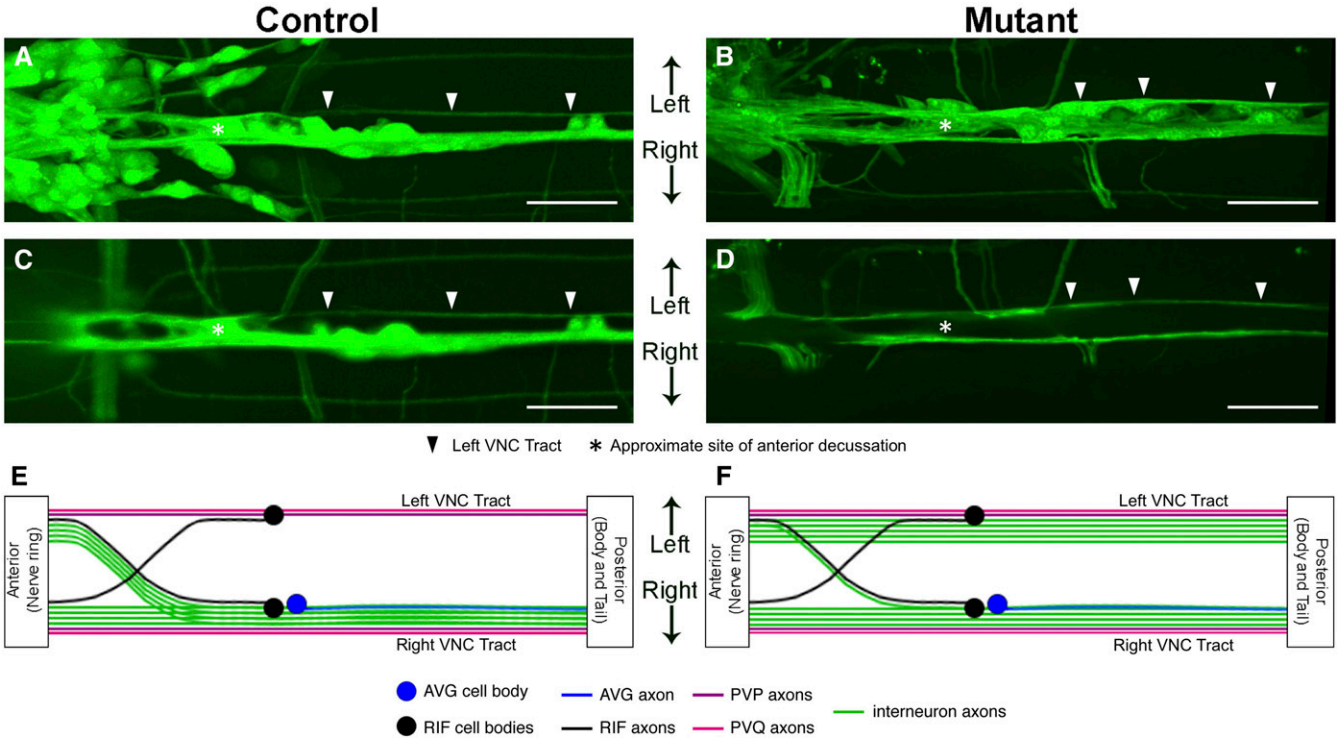

Figure 1 Establishment of VNC asymmetry in control animals and asymmetry defects in mutant animals. (A and C) In control animals (wild type) axons cross into the right axon tract at the anterior decussation point (*). This establishes the asymmetry of the VNC with the majority of axons in the right axon tract and only a few axons in the left axon tract (▾). (A) Shows a projection of all focal planes; (C) shows a partial projection excluding focal planes containing most of the cell bodies to better illustrate the crossing of axons. (E) A schematic drawing showing selected neurons including the interneuron axons (green) that cross into the right axon tract. (B and D) In mutants with asymmetry defects [an *unc-34(hd132)* mutant animal is shown here], axons fail to cross into the right tract and continue to extend on the left side. This leads to a loss of the asymmetry. (B) Shows a projection of all focal planes; (D) shows a partial projection excluding focal planes containing cell bodies to better illustrate the failure of axons to cross. (F) A schematic drawing showing selected neurons including the interneuron axons (green) that fail to cross into the right axon tract. Anterior is to the left in all images. Marker used: *rgef-1*::*GFP*. Bar, 15 μm.

Following EMS exposure, animals were allowed to recover for 4 hr after which 15 healthy looking L4 animals were transferred to 150 mm × 15 mm agar plates seeded with *Escherichia coli* OP50. For nonclonal screens, plates were cultured until food was used up at the early F_2 stage. At this point, plates were divided into large sections, plated on new 150 mm × 15 mm NGM plates and grown overnight at 20°. The plates were screened for individuals displaying VNC asymmetry defects under a high-resolution dissecting microscope (Kramer Scientific, Yonkers, NY). The *rol-6* phenotype facilitated the identification of mutant animals. Animals with defects were isolated and allowed to reproduce. Approximately 92,000 animals were screened.

For clonal screens, individual F_1 animals were selected at random and placed on 60 mm × 15 mm NGM plates. Animals were then allowed to self-fertilize and the F_2 generation was examined for the presence of asymmetry defects as described above. A total of 7557 F_1 animals were screened.

SNP mapping and whole-genome sequencing

Following initial outcrossing, strains were crossed with CB4856 Hawaiian males for SNP mapping. Homozygous mutant F_2 animals were identified by their asymmetry defects and SNPs were identified as described (Wicks *et al.* 2001). Following initial SNP mapping, complementation tests were done for candidate genes where mutant strains were available.

Whole-genome sequencing (WGS) was done as described (Thompson *et al.* 2013). Briefly, sequencing was done on Illumina HiSeq instruments according to manufacturer's instructions. Sequence coverage was at least 20-fold. Sequences were processed, filtered, and compared to the reference genome sequence WS240. Only unique mutations in exons or at splice junctions were considered as candidate mutations. Sequencing was performed for *hd133* after outcrossing three times with N2 wild type.

Microscopy and characterization of axonal defects

VNC defects were analyzed in late-stage larvae and adult animals. Animals were incubated with 10 mM NaN_3 in M9 buffer for 1 hr and mounted on agar pads prior to analysis to prevent movement. Hermaphrodites were then scored using a 40× objective on a Zeiss Axioscope (Carl Zeiss AG). For scoring of axon navigation defects, axon trajectories were observed directly, individually drawn by hand, and then categorized. All phenotypic observation was performed on

Table 1 Alleles identified in genetic screens for VNC asymmetry defects

Allele	Gene	Asymmetry defects (%)[a]	Total VNC crossover defects (%)	Left-to-right VNC crossover defects (%)	Right-to-left VNC crossover defects (%)
Wild type	—	0	6	5	5
hd130	*col-99*	12***	59***	56***	40***
hd132	*unc-34*	22***	100***	80***	84***
hd133	*unc-52*	6***	24***	17***	20***

Penetrance of defects in single mutants is significantly different compared to wild type. *** $P < 0.001$ (χ^2 test). $n = 100$ for each phenotype scored.
[a] Percentage of animals showing at least partial loss of asymmetry of the VNC.

hermaphrodites and 100 animals were examined per genotype (unless noted otherwise). Due to the highly variable growth and reproduction rates of the mutant strains, we scored hermaphrodites in a nonblind fashion as animals reached maturity.

Confocal images were acquired on a Zeiss Axioplan II microscope connected to a Quorum WaveFX Spinning Disc system (Quorum Technologies, Puslinch, ON). Stacks of confocal images with 0.15- to 0.5-μm distance between focal planes were recorded. Image acquisition and analysis was carried out using Volocity software (Perkin-Elmer, Waltham, MA). Images in the figures are maximum intensity projections. Images for Figure 1 were deconvolved using Volocity's iterative deconvolution algorithm with a calculated point spread function. Figures were assembled using Adobe Creative Suite CS5.1 (Adobe, San Jose, CA).

Statistical analysis

We used χ^2 tests in Excel (Microsoft, Redmond, WA) to determine the statistical significance of differences in phenotypes. Multiple comparisons in Table 3 were corrected by a Bonferroni correction, where the given α value was divided by the number of comparisons (n) made; therefore, for statistical significance in multiple comparisons individual P-values are $\leq \alpha/n$.

Data availability

Strains are available upon request. The authors affirm that all data necessary for confirming the conclusions of the article are present within the article, figures, and tables.

Results

Identification of mutants leading to a symmetrical ventral cord

We performed both clonal and nonclonal screens to identify mutants that fail to establish an asymmetrical VNC. For the nonclonal screens, we directly screened F_2 progeny of mutagenized P_0 individuals, which were grown in large numbers together. The nonclonal screens were designed to identify recessive mutations leading to highly penetrant asymmetry defects without affecting other aspects of development. This form of screening is less well suited to identifying mutations causing weakly penetrant defects or to isolating mutations that have additional defects that negatively affect overall development and growth of the animal. From the nonclonal screens only one mutation, *hd130*, was isolated (Table 1). We therefore switched to clonal screens, where we isolated F_1 individuals. This should allow the identification of mutants with weakly penetrant defects and mutants that grow more slowly than wild type. Clonal screens are much more time consuming, resulting in a much smaller number of individuals that can be screened. Two alleles, *hd132* and *hd133*, were isolated in clonal screens. All three alleles led to weakly penetrant asymmetry defects ranging from 8 to 22% (Figure 2 and Table 1). The asymmetry defects were caused by a failure of axons to cross into the right VNC axon tract at the anterior end of the VNC. In most mutant animals, some axons still did cross into the right tract so that asymmetry was not completely lost. In addition, all alleles showed crossing of axons between left and right axon tracts along the entire length of the VNC (Figure 2 and Table 1), indicating that navigation defects were not limited to the initial crossing at the anterior end of the VNC. Defects varied from animal to animal and not every animal showed all types of crossover defects.

We used WGS, SNP mapping, and complementation tests to characterize the genes. *hd130* is an allele of *col-99*, encoding a transmembrane collagen similar to the transmembrane collagen types XIII, XXIII, and XXV in vertebrates (Taylor *et al.* 2018). Sequencing of *hd130* revealed an early nonsense mutation predicted to truncate the protein after 24 amino acids (Figure 3).

hd132 was identified as an allele of *unc-34*, encoding the actin modulator Enabled (Ena)/Vasodilator-stimulated phosphoproteins (VASP). Complementation tests with unc-34(e556) revealed 10% asymmetry defects in *unc-34(hd132)/unc-34(e556)* transheterozygotes ($n = 50$). Sequencing of *unc-34(hd132)* coding regions revealed a guanine to adenine base pair change, changing a tryptophan into a stop codon within the predicted VASP domain (Figure 3). The introduced stop codon results in a truncation of the protein after 366 amino acids, removing the final 102 amino acids of the largest isoform UNC-34a (Figure 3). *unc-34* is predicted to encode eight isoforms (a–h). *unc-34(hd132)* affects predicted isoforms a, d, e, f, and g, but not the shorter isoforms b and c. Defects in *unc-34(hd132)* are slightly higher than in the canonical allele, *unc-34(e556)*, which has 15% asymmetry defects.

hd133 was identified as an allele of *unc-52*, encoding the basement membrane protein perlecan. Complementation tests with *unc-52(gk3)* revealed 4% asymmetry defects in *unc-52(hd133)/unc-52(gk3)* transheterozygotes ($n = 78$).

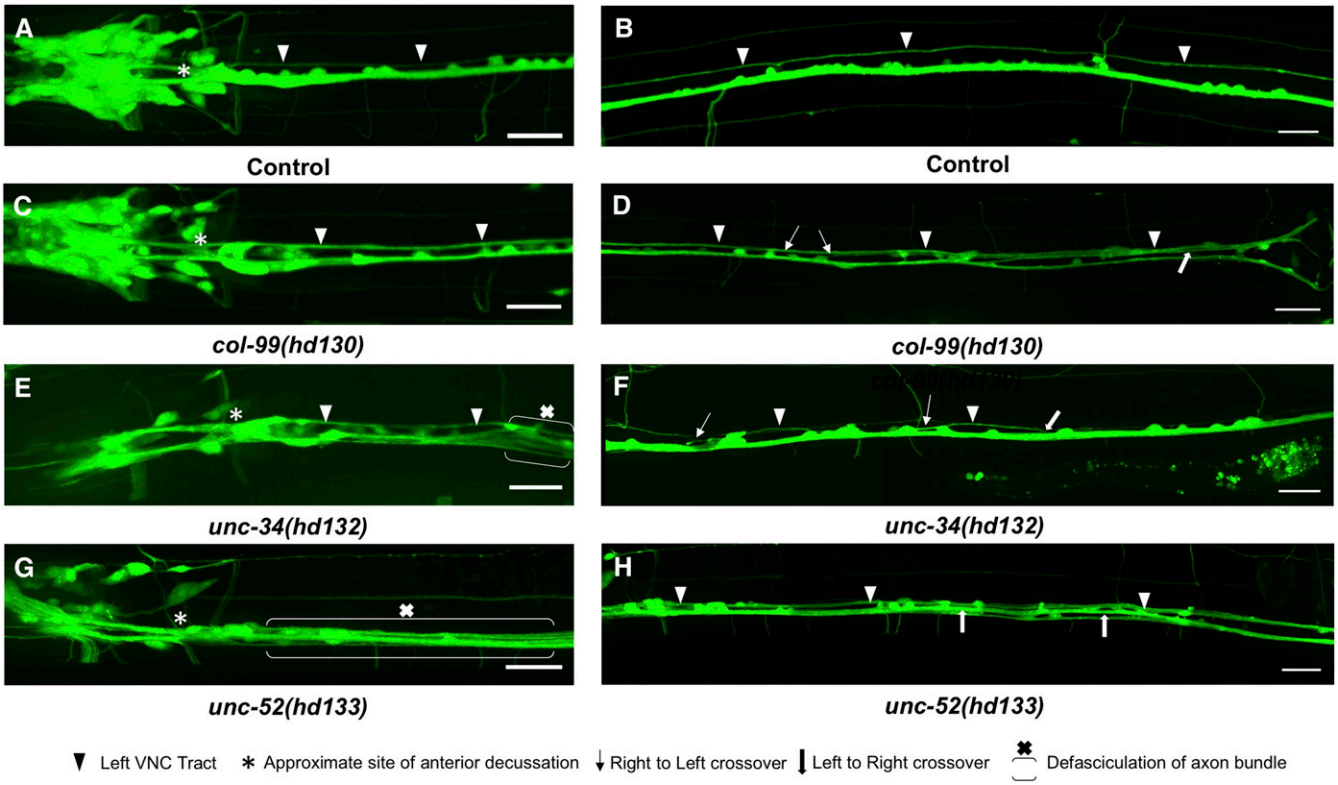

Figure 2 Axon navigation defects in *unc-34*, *col-99*, and *unc-52* mutants. (A, C, E, and G) depict the anterior part of the VNC with the normal decussation point (*). (B, D, F, and H) Show a region of the VNC posterior to the decussation point. (A and C) Control animals (wild type) show normal crossing of axons at the decussation point (A) and no midline crossing in the VNC (B). (C and D) In *col-99(hd130)* mutants, some axons fail to cross into the right tract and remain on the left side (C). In addition, axons cross the midline along the VNC (D). (E and F) *unc-34(hd132)* mutant animals show defects as described for *col-99(hd130)*. In addition, the right VNC is often defasciculated as shown in (E); region marked with the bracket. (G and H) Similar midline crossing and fasciculation defects are also found in *unc-52(hd133)* mutants. Anterior is to the left in all images. Marker used: *rgef-1*::*GFP*. Bar, 15 μm.

Sequencing revealed a guanine to adenine missense mutation in *unc-52(hd133)*, leading to a cysteine to tyrosine change at amino acid 723 of UNC-52E (Figure 3). This falls within a predicted laminin EGF-like domain (LE domain) common to most isoforms of UNC-52.

Screening candidate genes for defects in VNC asymmetry

Our genetic screens did not identify mutations with highly penetrant VNC asymmetry defects. In addition, the screens identified alleles of known axon guidance genes. We therefore tested mutants in genes of known axon guidance pathways as well as selected basement membrane components for potential asymmetry defects.

We tested mutants in three basement membrane components: *nid-1* (nidogen), *epi-1* (laminin-α), and *unc-52* (perlecan). We found that mutations in all three genes cause minor but significant asymmetry defects. The penetrance of these defects was 11% in *nid-1(cg119)* (Figure 4B and Table 2), 13% in *epi-1(rh200)*, and 6% in *unc-52(gk3)* mutant animals (Table 2). In contrast to *nid-1(cg119)*, which is a putative null allele, both *epi-1(rh200)* and *unc-52(gk3)* are partial loss-of-function alleles, since null alleles in these genes are not viable. *unc-52(gk3)* affects only two of the 16 splice variants (*unc-52e* and *unc-52g*). We tested a second allele, *unc-52(e444)*, which is a nonsense allele removing the C-terminal EGF and LG domains as well as several immunoglobulin domains affecting 11 splice variants including *unc-52e* but not *unc-52g*. *unc-52(e444)* mutant animals do not show any asymmetry defects, suggesting that only some isoforms of UNC-52 have a role in establishing VNC asymmetry.

Since we identified a *col-99* allele in our screens, we tested the putative receptors of *col-99*, *ddr-1*, and *ddr-2*. Mutations in *ddr-1* and *ddr-2* single mutants produce either no (*ddr-1*) or only minor VNC asymmetry defects of 4% in the case of *ddr-2* (Table 2). However, *ddr-1 ddr-2* double mutants show increased defects of 11% penetrance, similar to those seen in *col-99* mutants. *unc-6* encodes netrin, a major guidance cue for axons navigating in the dorsoventral direction. In 11% of *unc-6(ev400)* mutant animals, VNC asymmetry is disrupted (Table 2). Loss of the netrin receptors UNC-40 or UNC-5 resulted in slightly lower penetrance of defects at 5 and 9%, respectively (Table 2). Loss of Robo receptor homolog SAX-3 in *sax-3(ky123)* mutant animals results in slightly higher penetrant defects at 16% (Table 2). *sax-3* encodes the receptor for *slt-1*. However, previously we found that

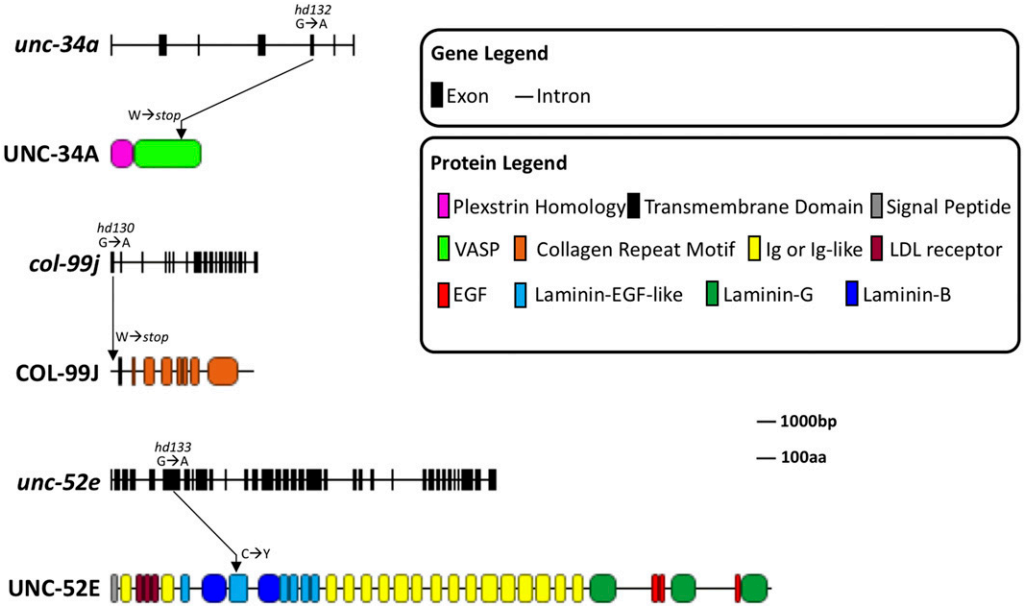

Figure 3 Nature and location of the mutations isolated in the genetic screens. Gene and protein models for *unc-34*, *col-99*, and *unc-52*. The location of the mutations in *unc-34(hd132)*, *col-99(hd130)*, and *unc-52(hd133)* is indicated. The consequences of the mutations at the amino acid level are shown as well. For all models the longest predicted splice isoforms were used. Ig, immunoglobulin.

slt-1(eh15) mutant animals do not have VNC asymmetry defects (Hutter 2003), suggesting that *slt-1* is not the ligand of *sax-3* in this case. *vab-1* encodes the sole ephrin receptor in *C. elegans*. *vab-1(dx31)* mutant animals display only minor VNC asymmetry defects at 4% (Table 2).

Several axon guidance pathways converge on *unc-34*, encoding the actin modulator Ena/VASP, and *unc-73*, encoding a guanine nucleotide exchange factor (GEF) (Trio homolog) for the small G proteins Rac and ρ. As described earlier, *unc-34(hd132)* mutant animals have 22% penetrant VNC asymmetry defects (Table 1). Alleles affecting ρ- [*unc-73 (ev802)*] and Rac-specific [*unc-73(rh40)*] isoforms of *unc-73* cause 5 and 6% asymmetry defects, respectively (Table 2).

Taken together, we found that mutations in several basement membrane components and known axon guidance genes have VNC asymmetry defects. None of the mutants have penetrant defects, suggesting that the establishment of VNC asymmetry is redundantly controlled by several pathways.

VNC asymmetry defects in a nid-1 mutant background

We recently discovered that *nid-1(cg119)* substantially enhances navigation defects of the AVG axon when combined with certain mutations that on their own have little to no AVG navigation defects (Bhat and Hutter 2016). This suggests that mutations in *nid-1* compromise the environment within which the AVG axon extends, revealing partially redundant functions of genes in AVG axon navigation which may influence other VNC axons as well. We therefore systematically generated double mutants with *nid-1* to test whether synergistic effects also exist for the establishment of overall VNC asymmetry.

col-99(hd130); *nid-1(cg119)* double mutants did not show a significant increase in asymmetry defects over either single mutant, 14 *vs.* 12 and 11%, respectively. This suggests both genes likely function in the same pathway in establishment of VNC asymmetry (Table 3). A *nid-1*; *ddr-1 ddr-2* triple mutant likewise failed to display an increased penetrance of defects over the *nid-1* single or the *ddr-1 ddr-2* double mutant animals (Table 3). This result suggests *nid-1* also functions in the same pathway as *ddr-1* and *ddr-2*. Double mutants of *nid-1* with *vab-1* or *unc-52* also showed no significant enhancement over the *nid-1* single mutants (Table 3). However, since the penetrance of defects in *unc-52* and *vab-1* single mutants is very low, an additive effect is difficult to detect.

On the other hand, *nid-1*; *sax-3* double mutants showed a significant increase in VNC asymmetry defects compared to the corresponding single mutants. Here, defects increased from 17% in *sax-3* mutant animals to 27% in *sax-3 nid-1* double mutants. *nid-1*; *unc-6* double mutant animals display defects of 37%, a synergistic enhancement greater than the combination of each single mutant of 6 and 11%, respectively. UNC-6/netrin receptors (UNC-5 and UNC-40) fail to show a significant enhancement in *nid-1* double mutants (Table 3). This suggests that the receptors might act redundantly. *unc-34 nid-1* double mutants also show a synergistic enhancement of defects, increasing from 22% in *unc-34* mutant animals to 58% in double mutant animals (Table 3). *epi-1*; *nid-1* double mutants also showed a synergistic enhancement of VNC defects to nearly 30% (Table 3). Taken together, several single mutants (*unc-6*, *unc-34*, *epi-1*) with weakly penetrant VNC asymmetry defects show synergistic effects when placed in a *nid-1* mutant background. Our analysis also showed that *nid-1*, *col-99*, *ddr-1*, and *ddr-2* act in the same pathway.

At least four different genetic pathways control VNC asymmetry

Our *nid-1* double mutant analysis suggests that several pathways acting in parallel establish VNC asymmetry. To test the extent to which redundantly acting pathways contribute to

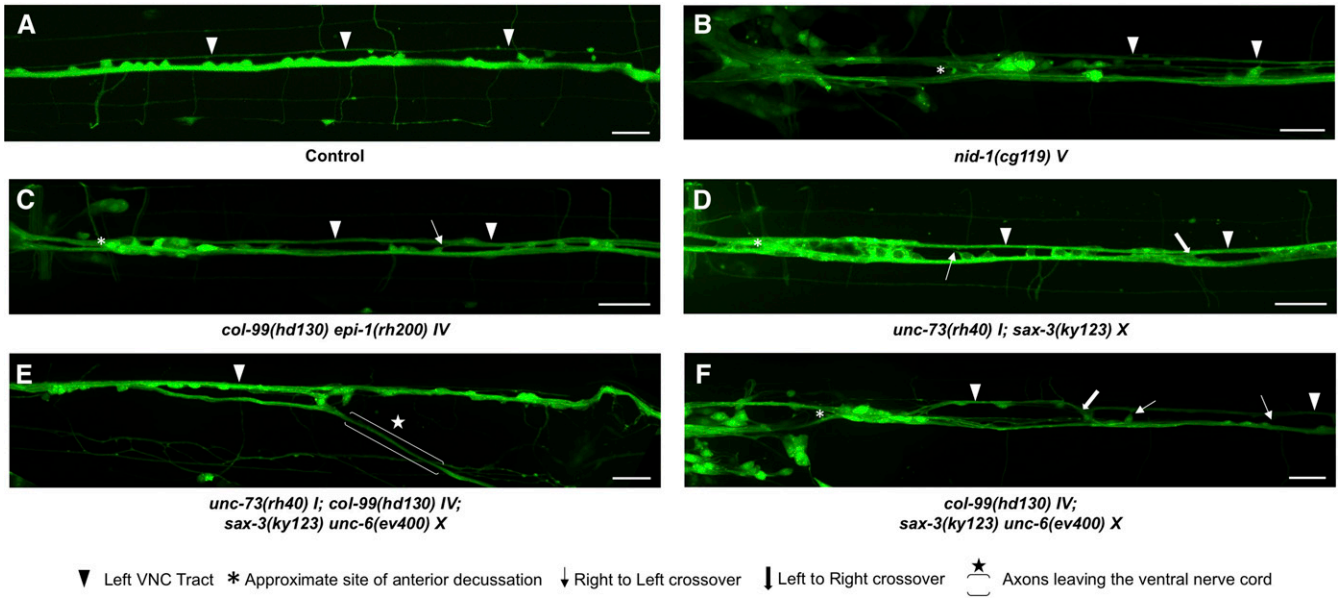

Figure 4 Examples of VNC asymmetry and axon navigation defects in selected mutant combinations. (A) Control animal (wild type). Most axons extend in the right VNC tract. (B) In *nid-1(cg119)* mutants, some axons fail to cross into right tract and instead extend in left VNC tract. (C) In *col-99(hd130) epi-1(rh200)* double mutants, some axons initially fail to cross into right ventral tract and remain in the left tract. In addition, some axons cross from the right to the left tract. (D) Similar defects are found in *unc-73(rh40)*; *sax-3(ky123)* double mutants. Here axons are also found to cross from the left into the right tract. (E) In *unc-73(rh40)*; *col-99(hd130)*; *unc-6(ev400) sax-3(ky123)* quadruple mutants, axons sometimes leave the VNC altogether. (F) *col-99(hd130)*; *unc-6(ev400) sax-3(ky123)* triple mutants show variable defects including left-to-right and right-to-left midline crossing defects. Anterior is to the left in all images. Marker used: *rgef-1*::*GFP*. Bar, 15 μm.

the establishment of VNC asymmetry, loss-of-function mutations in selected genes (*col-99*, *unc-73*, *sax-3*, *unc-6*, and *epi-1*)—likely representing different pathways—were combined and analyzed for VNC asymmetry defects (Figure 4 and Table 4).

All double mutants with *col-99* showed additive and occasionally synergistic enhancement of VNC asymmetry defects over any single mutant (Table 4). *col-99 epi-1* double mutants show the greatest penetrance of defects with 40% of animals displaying loss of normal VNC asymmetry (Figure 4C and Table 4) compared to 14% in *epi-1* animals, an increase of 26%. Hence all tested genes appear to function in VNC signaling pathways parallel to *col-99*. Loss of UNC-6/netrin on its own results in 13% of animals displaying VNC asymmetry defects, which is synergistically enhanced in all double mutant combinations (Table 4). *col-99*; *unc-6* double mutants resulted in the lowest penetrance of the double mutants with 35% and *sax-3 unc-6* animals the highest at 52% (Table 4). Thus *unc-6* represents a separate genetic pathway for guidance of axons into the right VNC axon tract. *sax-3* also represents a parallel pathway for this process with all double mutants significantly enhancing defects compared to single mutants (Table 4). Enhancement of defects was synergistic for *unc-73*; *sax-3* and *sax-3 unc-6* double mutants, and additive for *col-99*; *sax-3* and *epi-1*; *sax-3* animals (Table 4). The basement membrane component EPI-1 affects VNC asymmetry establishment independently from *sax-3*, *unc-6*, and *col-99*; as VNC defects were significantly enhanced in all three double mutant combinations (Table 4). A double mutant of *unc-73*; *epi-1* however did not show significant enhancement of defects over an *epi-1* single mutant, indicating they act in the same pathway.

We generated triple mutant strains with combinations of the above genes to test whether this further increases the penetrance of VNC asymmetry defects compared to double mutant strains. *unc-73*; *col-99*; *sax-3* triple mutants display 68% penetrant VNC asymmetry defects. This is vastly greater than any of the double mutant combinations of these genes (27, 31, and 39%; Table 4) and confirms the genes function in parallel pathways here. Combining *unc-73* mutations with *col-99* and *unc-6* mutations likewise results in increased penetrance (64%) over all double mutants (Table 4). *unc-73*; *epi-1*; *unc-6* and *unc-73*; *epi-1*; *sax-3* triple mutants also showed highly penetrant VNC asymmetry defects with 66 and 61% penetrance, respectively. These results are also significantly higher than any comparable double mutant animal (Table 4). *col-99 epi-1*; *unc-6* triple mutants display 57% VNC asymmetry defects, significantly enhanced relative to the strongest double mutant strain *col-99 epi-1* (Table 4). *col-99 epi-1*; *sax-3* mutants display VNC asymmetry defects in 61% of animals, also significantly higher than 40% observed for *col-99 epi-1* mutant animals. *unc-73*; *col-99 epi-1* triple mutant animals display VNC asymmetry in 42% of animals examined (Table 4). This was significantly higher than both *unc-73*; *col-99* (27%) and *unc-73*; *epi-1* (21%) double mutants but not higher than *unc-73*; *epi-1* (40%). *col-99*; *sax-3 unc-6* triple mutants showed significant enhancement of VNC defects (54%) compared to *col-99*; *sax-3* (31%) and *col-99*; *unc-6* animals (35%), but no difference compared to *sax-3 unc-6* double mutants

Table 2 VNC asymmetry defects in known axon guidance genes

Genotype	Gene product	Asymmetry defects (%)[a]
Wild type		0
Basement membrane components		
nid-1(cg119) V	nidogen	11***
epi-1(rh200) IV	laminin	13***
unc-52(gk3) II	perlecan	6*
unc-52(e444) II	perlecan	0
Guidance cues and receptors		
col-99(hd130) IV	Transmembrane collagen	12**
ddr-1(ok874) X	Collagen receptor	0
ddr-2(ok574) X	Collagen receptor	4*
ddr-1 ddr-2 X	Collagen receptors	11***
unc-6(ev400) X	netrin; axon guidance cue	11***
unc-5(e53) IV	Receptor for UNC-6	9**
unc-40(e271) I	Receptor for UNC-6	5*
sax-3(ky123) X	Receptor for guidance cue (Slit)	16***
vab-1(dx31) II	Ephrin receptor	4*
Intracellular proteins		
unc-73(ev802) I	GEF for Rho	5*
unc-73(rh40) I	GEF for Rac	6*
unc-34(hd132) V	Ena/VASP; actin modulator	22***

Penetrance of defects in single mutants is significantly different compared to wild type. * $P < 0.05$, ** $P < 0.01$, *** $P < 0.001$ (χ^2 test). $n = 100$ for each mutant.
[a] Percentage of animals showing at least partial loss of asymmetry of the VNC.

(Table 4). Finally, the triple mutant of *unc-73*; *sax-3 unc-6* displays VNC asymmetry defects in 47% of animals. This is not a significant increase over the double mutant combinations (Table 4). It appears *sax-3* and *unc-6* represent parallel pathways with *unc-73* acting in both of them.

A quadruple mutant containing *unc-73*, *col-99*, *sax-3*, and *unc-6* was created to see if the penetrance of defects could be further increased. However, the penetrance of defects in this quadruple mutant was 66%, comparable to penetrance found in the corresponding triple mutants (Table 4). We were not able to generate a *col-99 epi-1*; *sax-3 unc-6* quadruple mutant, suggesting that this mutant combination is not viable. *unc-34* is implicated in several axon guidance pathways and showed a strong synergistic effect together with *nid-1*. We therefore generated a *col-99*; *unc-34*; *sax-3* and *unc-6* quadruple mutant to see if we could further enhance the penetrance of defects. We found 78% penetrant asymmetry defects in this quadruple mutant, the highest penetrance of defects in any triple or quadruple mutant combination. Taken together, these results identify four different pathways (represented by *col-99*, *unc-6*, *sax-3*, and *epi-1*) that act together to control VNC asymmetry (Figure 5). The penetrance of the defects in the strongest quadruple mutant approaches 80%, which suggests that these genes represent important pathways establishing VNC asymmetry.

Discussion

Genes identified in the genetic screens

In our genetic screens, we identified alleles of three genes with partially penetrant VNC asymmetry defects, implicating these genes in the establishment of VNC asymmetry. The most penetrant defects were found in *hd132*, which is an allele of *unc-34* (Ena/VASP). Ena/VASP proteins bind actin, preventing binding of capping proteins and thereby allowing for rapid extension of the actin filaments (Yang and Svitkina 2011). Ena/VASP proteins are essential for filopodia formation in the growth cone in response to guidance cues. In *C. elegans*, UNC-34 is well characterized for its role in the downstream signaling pathways of several known guidance cues. *unc-34* was previously shown to act downstream of *slt-1*, and with *sax-3*, in AVM axon navigation (Yu *et al.* 2002). Further analysis found that *unc-34* also affects AVM navigation downstream of *unc-6* through interactions with the netrin receptor UNC-40 (Gitai *et al.* 2003). Here UNC-40 recruits parallel signaling pathways for proper extension of AVM axons, one associated with UNC-34 signaling and another with CED-10 (Yu *et al.* 2002; Gitai *et al.* 2003). In vertebrates, loss of Ena/VASP is associated with defects in axon tract formation of the CNS and PNS, and commissure formation in the forebrain (Lanier *et al.* 1999; Menzies *et al.* 2004). The *unc-34(hd132)* nonsense mutation is predicted to disrupt the C-terminal VASP domain. The VASP domain is associated with actin filament binding and is important in facilitating quick processing of actin filament extension (Bachmann *et al.* 1999; Ferron *et al.* 2007; Hansen and Mullins 2010). In addition, the VASP domain is essential for normal tetramerization of the mature protein (Bachmann *et al.* 1999; Kühnel *et al.* 2004). *unc-34(hd132)* therefore likely represents a strong loss-of-function allele. Two shorter isoforms of *unc-34* that lack the VASP domain would not be affected in *unc-34(hd132)*. It is therefore possible that *unc-34(hd132)* retains some function. Taken together, *unc-34(hd132)* represents a novel allele of *unc-34* in *C. elegans* that establishes a role of Ena/VASP proteins in axonal guidance at the anterior end of the VNC to establish an asymmetrical VNC.

Another mutation isolated in the screen, *hd133*, is an allele of *unc-52*, which encodes the sole perlecan homolog in *C. elegans*. Perlecan is a large heparan sulfate proteoglycan (HSPG) found abundantly in the basement membrane. Mutations in *unc-52* lead to defects in myofilament assembly and a failure of the myofilament lattice to attach to the muscle cell membrane (Rogalski *et al.* 1995, 2001). In addition to its roles in muscle formation and attachment, UNC-52 also functions in axon migration in *C. elegans* (Yang *et al.* 2014). Loss of *unc-52* causes misplacement of guidance cues in the basement membrane, in particular of UNC-6/netrin. This in turn changes the orientation of netrin receptors on outgrowing growth cones. Specifically, UNC-40/DCC receptors appear to mislocalize on growth cones of HSN axons in *unc-52* mutant animals (Yang *et al.* 2014). This causes variations in outgrowth patterns of HSN axons which gain a bias toward anterior and posterior axon extension as opposed to ventral extension in wild-type animals (Yang *et al.* 2014). UNC-52 similarly functions in axon guidance of NSM neurons where its loss is associated with misdirection and early termination (Axäng *et al.* 2008). UNC-52 is also one of two HSPGs

Table 3 VNC asymmetry defects in double mutants between *nid-1* and known axon guidance genes

Genotype	Gene product	Asymmetry defects (%)[a]
nid-1(cg119)		11
	nidogen	
Basement membrane components		
nid-1(cg119); epi-1(rh200)	laminin	27*
nid-1(cg119); unc-52(gk3)	perlecan	20
nid-1(cg119); unc-52(e444)	perlecan	13
Guidance cues and receptors		
nid-1(cg119); col-99(hd130)	Transmembrane collagen	14
nid-1(cg119); ddr-1(ok874)	Collagen receptor	12
nid-1(cg119); ddr-2(ok574)	Collagen receptor	13
nid-1(cg119); ddr-1 ddr-2	Collagen receptors	14
nid-1(cg119); unc-6(ev400)	netrin; axon guidance cue	37**
nid-1(cg119); unc-5(e53)	Receptor for UNC-6	16
nid-1(cg119); unc-40(e271)	Receptor for UNC-6	19
nid-1(cg119); sax-3(ky123)	Receptor for guidance cue (Slit)	27*
nid-1(cg119); vab-1(dx31)	Ephrin receptor	16
Intracellular proteins		
nid-1(cg119); unc-73(ev802)	GEF for Rho	21
nid-1(cg119); unc-73(rh40)	GEF for Rac	26
nid-1(cg119); unc-34(hd132)	Ena/VASP; actin modulator	58**

Penetrance of defects in *nid-1* double mutants is significantly different compared to *nid-1* single mutants after Bonferroni correction with * 95% confidence interval or ** 99% confidence interval (χ^2 test). n = 100 for each mutant combination scored.
[a] Percentage of animals showing at least partial loss of asymmetry of the VNC.

involved in branching of AIY neuron axons (Díaz-Balzac *et al.* 2014). *unc-52(hd133)* causes a missense mutation changing a cysteine to tyrosine of amino acid 723. *unc-52(gk3)*, which has asymmetry defects similar to *unc-52(hd133)*, only affects isoforms *unc-52e* and *unc-52g*, suggesting that one or both of these isoforms specifically are required for VNC asymmetry. *unc-52(e444)*, which affects most isoforms including *unc-52e* but not *unc-52g*, shows no asymmetry defects, suggesting that *unc-52g* is the relevant isoform. However, *unc-52g* would not be affected by *unc-52(hd133)*, which affects most other isoforms. This points toward a more complex requirement of different isoforms to establish VNC asymmetry.

A third mutation identified in the screens, *hd130*, is an allele of *col-99*, encoding a transmembrane collagen. Our recent description of the role of *col-99* in axon guidance in *C. elegans* (Taylor *et al.* 2018) is largely based on the allele isolated here. We have recently shown that *col-99* mutants have axon guidance defects in several classes of axons in the VNC, including the command interneurons of the motor circuit. These frequently cross into the left VNC axon tract in *col-99* mutants. We showed that the extracellular domain of COL-99 is likely to be cleaved and released from the cell surface (Taylor *et al.* 2018). COL-99 most likely acts as a ligand for the discoidin domain receptors (DDRs) DDR-1 and DDR-2, which are expressed in neurons showing axonal navigation defects.

Taken together our screens identified a small number of mutations in genes contributing to the establishment of VNC asymmetry. The observation that none of the mutants identified in the screen has highly penetrant asymmetry defects suggests that several pathways act together to ensure the correct formation of the left and right VNC axon tracts.

The role of known axon guidance genes in the establishment of VNC asymmetry

Our screens for novel mutants with a role in the establishment of VNC asymmetry identified a small number of novel alleles with weakly penetrant defects, mostly in previously characterized genes. This raised the possibility that other known guidance genes might contribute to the establishment of VNC asymmetry. We tested genes from the netrin (*unc-6*, *unc-5*, *unc-40*), ephrin (*vab-1*), Slit/Robo (*sax-3*), and DDR signaling pathways (*col-99*, *ddr-1*, *ddr-2*) and downstream effectors (*unc-73*, *unc-34*) as well as genes encoding basement membrane proteins (*nid-1*, *epi-1*, *unc-52*) that may act indirectly for a role in establishing VNC asymmetry. Most of the mutants had some asymmetry defects in the range of 4–16% but none of them had penetrant defects that were higher than those in *unc-34* mutants at 22%. This suggests that a combination of known guidance cues contributes to the establishment of VNC asymmetry.

Nidogens are monomeric glycoproteins found in the basement membrane. In vertebrates, nidogens bind a large variety of other membrane components (Mayer *et al.* 1993; Pöschl *et al.* 1994). In mammals, nidogen mutants are viable, suggesting that nidogen is not a structural component essential for the integrity of basement membranes (Murshed *et al.* 2000; Schymeinsky *et al.* 2002). In *C. elegans*, nidogen is encoded by the gene *nid-1*. *nid-1* mutant animals display defects in the navigation of VNC axons (Kim and Wadsworth 2000; Bhat and Hutter 2016) including an 11% VNC asymmetry defect penetrance. NID-1 is found in the basement membrane underlying the longitudinal axon tracts in *C. elegans* (Kang and Kramer 2000). It is possible that NID-1 binds guidance cues and other molecules, sequestering them

Table 4 VNC asymmetry defects in double, triple, and quadruple mutant combinations of known axon guidance genes

Genotype[a]	Asymmetry defects (%)[b]
Single mutants[c]	
col-99	12
epi-1	14
sax-3	17
unc-6	13
unc-34	22
unc-73	8
Double mutants[d]	
col-99 epi-1	40***
col-99; *sax-3*	31*
col-99; *unc-6*	35***
unc-73; *col-99*	27*
epi-1; *sax-3*	32*
epi-1; *unc-6*	38***
sax-3 unc-6	52***
unc-73; *epi-1*	21
unc-73; *sax-3*	39***
unc-73; *unc-6*	38***
Triple mutants[e]	
col-99; *epi-1*; *sax-3*	62**
col-99; *epi-1*; *unc-6*	57*
unc-73; *col-99*; *epi-1*	42
col-99; *sax-3 unc-6*	54
unc-73; *col-99*; *sax-3*	68***
unc-73; *col-99*; *unc-6*	64***
unc-73; *epi-1*; *sax-3*	61**
unc-73; *epi-1*; *unc-6*	66***
unc-73; *sax-3 unc-6*	47
Quadruple mutants	
unc-73; *col-99*; *sax-3 unc-6*	66
col-99; *unc-34*; *sax-3 unc-6*	78

* $P < 0.05$, ** $P < 0.01$, *** $P < 0.001$ (χ^2 test). n = 100 for each mutant combination scored.

[a] Alleles used are *unc-73(rh40)* I, *col-99(hd130)* IV, *epi-1(rh200)* IV, *unc-34(hd132)* V, *sax-3(ky123)* X, and *unc-6(ev400)* X.

[b] Percentage of animals showing at least partial loss of asymmetry of the VNC.

[c] Data for single mutants are copied from Table 2 and shown for comparison.

[d] For double mutants, penetrance of defects in double mutant is significantly different from the more penetrant single mutant.

[e] For triple mutants, penetrance of defects in triple mutant is significantly different from the more penetrant double mutant.

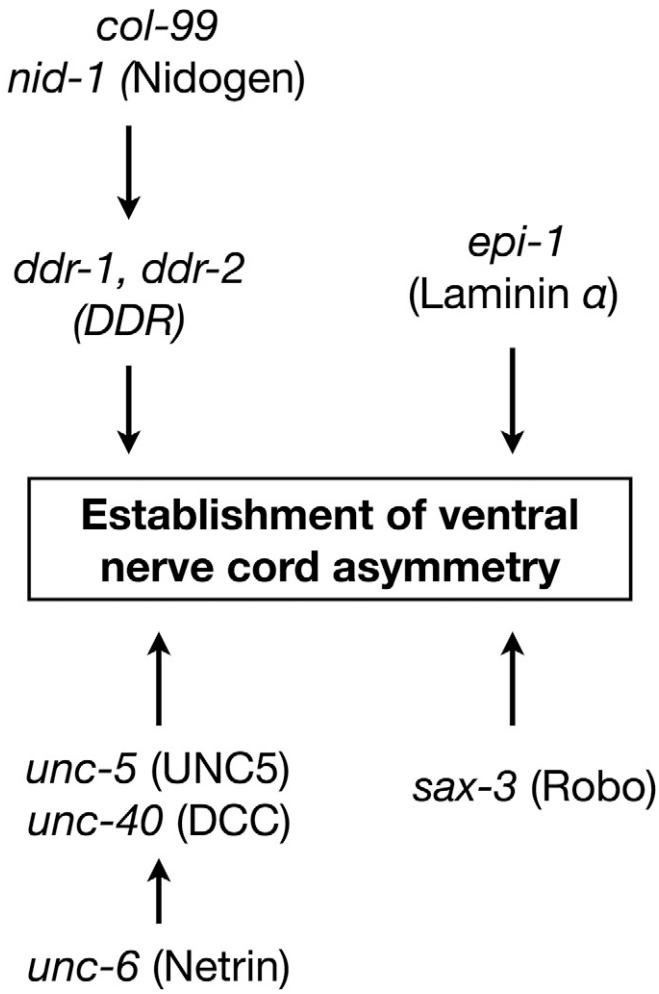

Figure 5 Model of genetic pathways contributing to the establishment of VNC asymmetry. We identified four independent pathways contributing to the establishment of VNC asymmetry.

within the basement membrane such that they are available to receptors on growth cones of outgrowing axons. We found that several mutants, showing no or weakly penetrant AVG axon navigation defects on their own, show synergistically enhanced defects in a *nid-1* mutant background. In addition, we found that *nid-1* acts in the same genetic pathway as *col-99* and *ddr-1/-2*, affecting VNC axon navigation, confirming our earlier observations (Taylor *et al.* 2018). None of the other genes tested conclusively functioned in a pathway with *nid-1*. However, some of the double mutant data (*e.g.*, for *unc-5*, *unc-40*, and *vab-1*) are inconclusive because additive effects cannot be clearly distinguished from no enhancement of defects compared to the single mutants due to the low penetrance of defects in the single mutants. Our data suggest that *unc-6* and *sax-3* act independently of *nid-1*. *epi-1*, *unc-73*, and *unc-34* also seem to act independently of *nid-1*. Taken together, the data suggest that only *col-99* and *ddr-1/-2* act in a pathway with *nid-1*, confirming our previous studies (Taylor *et al.* 2018), and that several genes (*unc-6*, *unc-34*, *epi-1*) show synergistic interactions with *nid-1*.

Genetic pathways controlling VNC asymmetry

To determine how many different genetic pathways contribute to VNC asymmetry, we evaluated asymmetry defects in double, triple, and quadruple mutants. We used *col-99*, *unc-73*, *sax-3*, *unc-6*, and *epi-1* as candidates likely representing separate and potentially redundant signaling pathways controlling the establishment of VNC asymmetry. *unc-6*, *col-99*, and *sax-3* encode guidance cues and receptors (Hedgecock *et al.* 1990; Ishii *et al.* 1992; Hao *et al.* 2001, p. 3; Taylor *et al.* 2018, p. 99). Combinations of null alleles of these genes in double and triple mutant animals suggest that all three genes act in different pathways (Figure 4). *col-99*; *unc-6 sax-3* triple mutants show >50% penetrant asymmetry defects, indicating these pathways provide a major input for VNC asymmetry.

unc-73 is a downstream effector acting in several axon guidance pathways (Chisholm *et al.* 2016). Our genetic

interaction data are largely consistent with *unc-73* acting simultaneously in the *sax-3* and *unc-6* pathways. *unc-73*; *sax-3* and *unc-73*; *unc-6* double mutants show additive defects compared to single mutants, but defects in double mutants are not further enhanced in the *unc-73*; *unc-6 sax-3* triple mutant. Interestingly, the genetic interaction data also suggest that *unc-73* acts in a pathway with *epi-1*, which is more difficult to interpret as *epi-1* encodes a structural component of the basement membrane.

epi-1/laminin α acts in parallel to the *col-99*, *unc-6*, and *sax-3* pathways, establishing a role for the basement membrane that is independent of these axon guidance pathways. The allele used in this study, *epi-1(rh200)*, represents a partial loss-of-function allele, since null alleles are embryonic lethal. This complicates the interpretation of double mutants. However, every mutant that was combined with *epi-1(rh200)* was a null allele, completely inactivating the corresponding genetic pathway. An enhancement of defects in *epi-1* double mutants can therefore still be taken as evidence that *epi-1* acts in a different pathway. Laminin is a structural component of basement membranes, which are substrates for axon extension but potentially also a source of basement membrane-embedded guidance cues. Therefore, in *epi-1(rh200)* mutants we cannot distinguish indirect effects of structural defects in the basement membrane from effects due to mislocalization of guidance cues. The fact that *epi-1* appears to act in parallel to the *col-99*, *unc-6*, and *sax-3* pathways suggests that these pathways are not compromised in *epi-1(rh200)* mutants.

Several different classes of neurons are involved in establishing VNC asymmetry. Currently we do not know whether the four different pathways we identified affect all classes of neurons in the same way or whether certain pathways are preferentially used by certain classes of neurons. A more detailed analysis with a panel of cell type-specific markers is required to address this question. If different classes of neurons use different pathways, the total number of pathways involved in establishing the VNC asymmetry could be substantially larger than the four we identified here.

The importance of VNC asymmetry

Almost all the axons in the VNC of *C. elegans* are found in the right axon tract despite an overall bilateral symmetry of the animals that includes almost all of the nervous system. The asymmetry is based on two kinds of guidance decisions during axon outgrowth. First of all, interneuron axons extending from the nerve ring into the VNC cross selectively from the left into the right axon tract at a defined crossing point at the anterior end of the VNC. Second, motor neuron axons, which extend from cell bodies located at the ventral midline, invariably extend into the right VNC axon tract. Interneuron axons establish synapses with motor neurons *en passant* within the VNC, which requires close contact between pre- and postsynaptic processes. Inhibitory motor neurons establish synapses with excitatory motor neurons also requiring close contact. Having all axons in one axon tract rather than in two separate tracts simplifies the overall circuit, which is not divided into separate left and right circuits. In *C. elegans*, muscle cells send extensions, called muscle arms, toward the VNC to establish neuromuscular junctions. Muscle cells on the left side have to extend their muscle arms over to the right side to gain access to the motor neuron axons in the right axon tract. Because of the small size of the animal—the left and right axon tract are ∼5 μm apart—this is not a major difficulty. Interestingly, muscle arms can localize and project to mispositioned motor neuron axons (Hedgecock *et al.* 1990), providing some flexibility in building the motor circuit. The fact that there are no separate left and right motor neurons means that left and right muscle cells receive the same innervation and are not able to contract independently. This is, in fact, an advantage considering that *C. elegans* moves by alternate contraction of dorsal and ventral muscles. Left and right muscles have to contract simultaneously and combining left and right circuits into one facilitates this.

In summary, in this study we identified four different genetic pathways that contribute to the establishment of the asymmetry of the VNC in *C. elegans*. The high degree of redundancy reflected by the low penetrance of defects in any single mutant made it difficult to identify the relevant genes in genetic screens. It is notable that, apart from *col-99*, all genes discussed here have been identified before as axon guidance factors. All genes have additional axon guidance functions, suggesting that guidance decisions required to establish asymmetry are not controlled by a unique set of genes dedicated specifically to this function. The penetrance of defects in the strongest quadruple mutant approached 80%, suggesting we identified several essential pathways controlling this process.

Acknowledgments

We thank members of the Hutter laboratory for discussions and comments on the manuscript. We thank the Moerman laboratory for performing the whole-genome sequencing and Stephane Flibotte for the bioinformatic analysis of the sequencing data. This work was supported by National Sciences and Engineering Research Council grant RGPIN-2017-03942 to H.H. Some strains used in this work were obtained from the *Caenorhabditis* Genetics Center (CGC), which is supported by the National Institutes of Health Office of Research Infrastructure Programs (P40 OD-010440).

Literature Cited

Alqadah, A., Y.-W. Hsieh, Z. D. Morrissey, and C.-F. Chuang, 2018 Asymmetric development of the nervous system. Dev. Dyn. Off. Publ. Am. Assoc. Anat. 247: 124–137. https://doi.org/10.1002/dvdy.24595

Axäng, C., M. Rauthan, D. H. Hall, and M. Pilon, 2008 Developmental genetics of the C. elegans pharyngeal neurons NSML and NSMR. BMC Dev. Biol. 8: 38. https://doi.org/10.1186/1471-213X-8-38

Bachmann, C., L. Fischer, U. Walter, and M. Reinhard, 1999 The EVH2 domain of the vasodilator-stimulated phosphoprotein mediates tetramerization, F-actin binding, and actin bundle formation. J. Biol. Chem. 274: 23549–23557. https://doi.org/10.1074/jbc.274.33.23549

Bauer Huang, S. L., Y. Saheki, M. K. VanHoven, I. Torayama, T. Ishihara *et al.*, 2007 Left-right olfactory asymmetry results from antagonistic functions of voltage-activated calcium channels and the raw repeat protein OLRN-1 in C. elegans. Neural Dev. 2: 24. https://doi.org/10.1186/1749-8104-2-24

Bhat, J. M., and H. Hutter, 2016 Pioneer axon navigation is controlled by AEX-3, a guanine nucleotide exchange factor for RAB-3 in Caenorhabditis elegans. Genetics 203: 1235–1247. https://doi.org/10.1534/genetics.115.186064

Brenner, S., 1974 The genetics of Caenorhabditis elegans. Genetics 77: 71–94.

Chang, S., R. J. Johnston, and O. Hobert, 2003 A transcriptional regulatory cascade that controls left/right asymmetry in chemosensory neurons of C. elegans. Genes Dev. 17: 2123–2137. https://doi.org/10.1101/gad.1117903

Chang, S., R. J. Johnston, C. Frøkjaer-Jensen, S. Lockery, and O. Hobert, 2004 MicroRNAs act sequentially and asymmetrically to control chemosensory laterality in the nematode. Nature 430: 785–789. https://doi.org/10.1038/nature02752

Chisholm, A. D., H. Hutter, Y. Jin, and W. G. Wadsworth, 2016 The genetics of axon guidance and axon regeneration in Caenorhabditis elegans. Genetics 204: 849–882. https://doi.org/10.1534/genetics.115.186262

Chuang, C.-F., M. K. Vanhoven, R. D. Fetter, V. K. Verselis, and C. I. Bargmann, 2007 An innexin-dependent cell network establishes left-right neuronal asymmetry in C. elegans. Cell 129: 787–799. https://doi.org/10.1016/j.cell.2007.02.052

Cochella, L., and O. Hobert, 2012 Embryonic priming of a miRNA locus predetermines postmitotic neuronal left/right asymmetry in C. elegans. Cell 151: 1229–1242. https://doi.org/10.1016/j.cell.2012.10.049

Díaz-Balzac, C. A., M. I. Lázaro-Peña, E. Tecle, N. Gomez, and H. E. Bülow, 2014 Complex cooperative functions of heparan sulfate proteoglycans shape nervous system development in Caenorhabditis elegans. G3 (Bethesda) 4: 1859–1870. https://doi.org/10.1534/g3.114.012591

Durbin, R. M., 1987 Studies on the Development and Organisation of the Nervous System of Caenorhabditis elegans. Ph.D. Thesis, University of Cambridge, Cambridge, UK.

Ferron, F., G. Rebowski, S. H. Lee, and R. Dominguez, 2007 Structural basis for the recruitment of profilin-actin complexes during filament elongation by Ena/VASP. EMBO J. 26: 4597–4606. https://doi.org/10.1038/sj.emboj.7601874

Gitai, Z., T. W. Yu, E. A. Lundquist, M. Tessier-Lavigne, and C. I. Bargmann, 2003 The netrin receptor UNC-40/DCC stimulates axon attraction and outgrowth through enabled and, in parallel, Rac and UNC-115/AbLIM. Neuron 37: 53–65. https://doi.org/10.1016/S0896-6273(02)01149-2

Hansen, S. D., and R. D. Mullins, 2010 VASP is a processive actin polymerase that requires monomeric actin for barbed end association. J. Cell Biol. 191: 571–584. https://doi.org/10.1083/jcb.201003014

Hao, J. C., T. W. Yu, K. Fujisawa, J. G. Culotti, K. Gengyo-Ando *et al.*, 2001 C. elegans slit acts in midline, dorsal-ventral, and anterior-posterior guidance via the SAX-3/Robo receptor. Neuron 32: 25–38. https://doi.org/10.1016/S0896-6273(01)00448-2

Hedgecock, E. M., J. G. Culotti, and D. H. Hall, 1990 The unc-5, unc-6, and unc-40 genes guide circumferential migrations of pioneer axons and mesodermal cells on the epidermis in C. elegans. Neuron 4: 61–85. https://doi.org/10.1016/0896-6273(90)90444-K

Hobert, O., 2014 Development of left/right asymmetry in the Caenorhabditis elegans nervous system: from zygote to postmitotic neuron. Genesis 52: 528–543. https://doi.org/10.1002/dvg.22747

Hobert, O., R. J. Johnston, and S. Chang, 2002 Left-right asymmetry in the nervous system: the Caenorhabditis elegans model. Nat. Rev. Neurosci. 3: 629–640. https://doi.org/10.1038/nrn897

Hutter, H., 2003 Extracellular cues and pioneers act together to guide axons in the ventral cord of C. elegans. Development 130: 5307–5318. https://doi.org/10.1242/dev.00727

Ishii, N., W. G. Wadsworth, B. D. Stern, J. G. Culotti, and E. M. Hedgecock, 1992 UNC-6, a laminin-related protein, guides cell and pioneer axon migrations in C. elegans. Neuron 9: 873–881. https://doi.org/10.1016/0896-6273(92)90240-E

Kang, S. H., and J. M. Kramer, 2000 Nidogen is nonessential and not required for normal type IV collagen localization in Caenorhabditis elegans. Mol. Biol. Cell 11: 3911–3923. https://doi.org/10.1091/mbc.11.11.3911

Kim, S., and W. G. Wadsworth, 2000 Positioning of longitudinal nerves in C. elegans by nidogen. Science 288: 150–154. https://doi.org/10.1126/science.288.5463.150

Kühnel, K., T. Jarchau, E. Wolf, I. Schlichting, U. Walter *et al.*, 2004 The VASP tetramerization domain is a right-handed coiled coil based on a 15-residue repeat. Proc. Natl. Acad. Sci. USA 101: 17027–17032. https://doi.org/10.1073/pnas.0403069101

Lanier, L. M., M. A. Gates, W. Witke, A. S. Menzies, A. M. Wehman *et al.*, 1999 Mena is required for neurulation and commissure formation. Neuron 22: 313–325. https://doi.org/10.1016/S0896-6273(00)81092-2

Mayer, U., R. Nischt, E. Pöschl, K. Mann, K. Fukuda *et al.*, 1993 A single EGF-like motif of laminin is responsible for high affinity nidogen binding. EMBO J. 12: 1879–1885. https://doi.org/10.1002/j.1460-2075.1993.tb05836.x

Menzies, A. S., A. Aszodi, S. E. Williams, A. Pfeifer, A. M. Wehman *et al.*, 2004 Mena and vasodilator-stimulated phosphoprotein are required for multiple actin-dependent processes that shape the vertebrate nervous system. J. Neurosci. 24: 8029–8038. https://doi.org/10.1523/JNEUROSCI.1057-04.2004

Murshed, M., N. Smyth, N. Miosge, J. Karolat, T. Krieg *et al.*, 2000 The absence of nidogen 1 does not affect murine basement membrane formation. Mol. Cell. Biol. 20: 7007–7012. https://doi.org/10.1128/MCB.20.18.7007-7012.2000

Pöschl, E., J. W. Fox, D. Block, U. Mayer, and R. Timpl, 1994 Two non-contiguous regions contribute to nidogen binding to a single EGF-like motif of the laminin gamma 1 chain. EMBO J. 13: 3741–3747. https://doi.org/10.1002/j.1460-2075.1994.tb06683.x

Rogalski, T. M., E. J. Gilchrist, G. P. Mullen, and D. G. Moerman, 1995 Mutations in the unc-52 gene responsible for body wall muscle defects in adult Caenorhabditis elegans are located in alternatively spliced exons. Genetics 139: 159–169.

Rogalski, T. M., G. P. Mullen, J. A. Bush, E. J. Gilchrist, and D. G. Moerman, 2001 UNC-52/perlecan isoform diversity and function in Caenorhabditis elegans. Biochem. Soc. Trans. 29: 171–176. https://doi.org/10.1042/bst0290171

Schymeinsky, J., S. Nedbal, N. Miosge, E. Pöschl, C. Rao *et al.*, 2002 Gene structure and functional analysis of the mouse nidogen-2 gene: nidogen-2 is not essential for basement membrane formation in mice. Mol. Cell. Biol. 22: 6820–6830. https://doi.org/10.1128/MCB.22.19.6820-6830.2002

Sulston, J. E., and H. R. Horvitz, 1977 Post-embryonic cell lineages of the nematode, Caenorhabditis elegans. Dev. Biol. 56: 110–156. https://doi.org/10.1016/0012-1606(77)90158-0

Sulston, J. E., E. Schierenberg, J. G. White, and J. N. Thomson, 1983 The embryonic cell lineage of the nematode Caenorhabditis elegans. Dev. Biol. 100: 64–119. https://doi.org/10.1016/0012-1606(83)90201-4

Taylor, J., T. Unsoeld, and H. Hutter, 2018 The transmembrane collagen COL-99 guides longitudinally extending axons in C. elegans. Mol. Cell. Neurosci. 89: 9–19. https://doi.org/10.1016/j.mcn.2018.03.003

Thompson, O., M. Edgley, P. Strasbourger, S. Flibotte, B. Ewing *et al.*, 2013 The million mutation project: a new approach to genetics in Caenorhabditis elegans. Genome Res. 23: 1749–1762. https://doi.org/10.1101/gr.157651.113

Troemel, E. R., A. Sagasti, and C. I. Bargmann, 1999 Lateral signaling mediated by axon contact and calcium entry regulates asymmetric odorant receptor expression in C. elegans. Cell 99: 387–398. https://doi.org/10.1016/S0092-8674(00)81525-1

Wadsworth, W. G., H. Bhatt, and E. M. Hedgecock, 1996 Neuroglia and pioneer neurons express UNC-6 to provide global and local netrin cues for guiding migrations in C. elegans. Neuron 16: 35–46. https://doi.org/10.1016/S0896-6273(00)80021-5

White, J. G., E. Southgate, J. N. Thomson, and S. Brenner, 1976 The structure of the ventral nerve cord of Caenorhabditis elegans. Philos. Trans. R. Soc. Lond. B Biol. Sci. 275: 327–348. https://doi.org/10.1098/rstb.1976.0086

White, J. G., E. Southgate, J. N. Thomson, and S. Brenner, 1986 The structure of the nervous system of the nematode Caenorhabditis elegans. Philos. Trans. R. Soc. Lond. B Biol. Sci. 314: 1–340. https://doi.org/10.1098/rstb.1986.0056

Wicks, S. R., R. T. Yeh, W. R. Gish, R. H. Waterston, and R. H. Plasterk, 2001 Rapid gene mapping in Caenorhabditis elegans using a high density polymorphism map. Nat. Genet. 28: 160–164. https://doi.org/10.1038/88878

Wood, W. B., 1991 Evidence from reversal of handedness in C. elegans embryos for early cell interactions determining cell fates. Nature 349: 536–538. https://doi.org/10.1038/349536a0

Wood, W. B., 1998 Handed asymmetry in nematodes. Semin. Cell Dev. Biol. 9: 53–60. https://doi.org/10.1006/scdb.1997.0189

Yang, C., and T. Svitkina, 2011 Filopodia initiation: focus on the Arp2/3 complex and formins. Cell Adhes. Migr. 5: 402–408. https://doi.org/10.4161/cam.5.5.16971

Yang, Y., W. S. Lee, X. Tang, and W. G. Wadsworth, 2014 Extracellular matrix regulates UNC-6 (netrin) axon guidance by controlling the direction of intracellular UNC-40 (DCC) outgrowth activity. PLoS One 9: e97258. https://doi.org/10.1371/journal.pone.0097258

Yu, T. W., J. C. Hao, W. Lim, M. Tessier-Lavigne, and C. I. Bargmann, 2002 Shared receptors in axon guidance: SAX-3/Robo signals via UNC-34/Enabled and a Netrin-independent UNC-40/DCC function. Nat. Neurosci. 5: 1147–1154. https://doi.org/10.1038/nn956

Communicating editor: H. Bülow